Application of neural network in metal adsorption using biomaterials (BMs): A review

Amrita Nighojkar[a†], Karl Zimmermann[b], Mohamed Ateia[c], Benoit Barbeau[d], Madjid Mohseni[b], Satheesh Krishnamurthy[e], Fuhar Dixit[b†*] and Balasubramanian Kandasubramanian[a*]

[a] Nano Surface Texturing Lab, Department of Metallurgical and Materials Engineering, Defence Institute of Advanced Technology (DU), Pune, India

[b] Department of Chemical and Biological Engineering, University of British Columbia, Vancouver, Canada

[c] United States Environmental Protection Agency, Cincinnati, USA

[d] Department of Civil, Geological and Mining Engineering, Polytechnique Montreal, Quebec, Canada

[e] School of Engineering & Innovation, The Open University, Milton Keynes, United Kingdom

† These authors contributed equally to this work.

* Corresponding author: meetkbs@gmail.com (B. Kandasubramanian) and fdixit@chbe.ubc.ca (F. Dixit)

Supplementary Information

Tables: 7

Figures: 10

S1. Physical and chemical modifications of biomaterial-based adsorbents

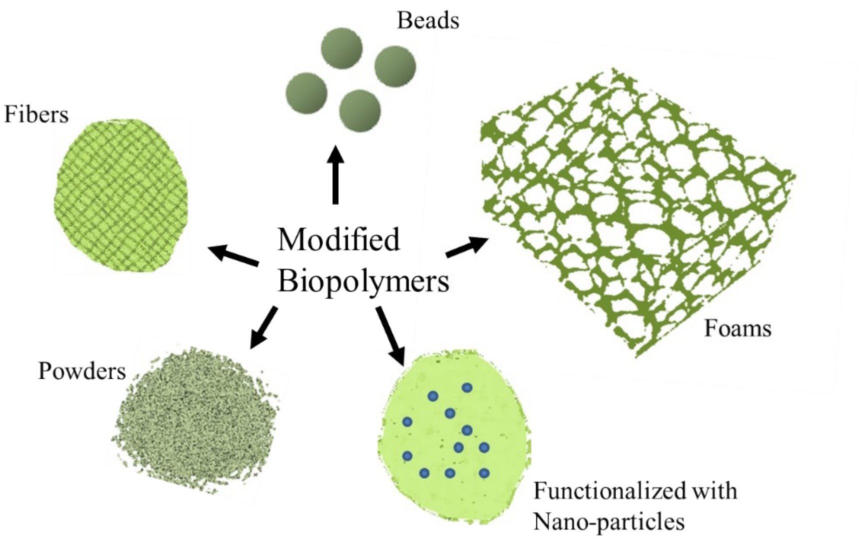

Fig.S1. A schematic depicting the physical and chemical modifications of biomaterial-based adsorbents.

S2. Experimental data range of input and output adsorption variables

Table S1. Range of experimental input and output adsorption variables used in modelling biomaterial batch adsorption systems (AD=Adsorbent dose, IC = Initial Concentration, AS = Agitation speed, T =Temperature, CT =Contact time, PS =Particle size, SA= Surface area, η = % removal or adsorption efficiency, AC =Adsorption capacity, ΔG = Gibbs free energy change, FC = final concentration, FpH = Final pH)

Metals adsorbed	Biomaterial	Independent Adsorption Variables									Dependent adsorption variables				Refernces
		AD	IC	pH	AS	T	CT	PS	SA	V	η	AC	pH/ FC	ΔG	
		g	mg/L		RPM	ºC	min	mm	m^2/g	mL	%	mg/g		KJ	
As (III)	Bacillus thuringiensis strain WS3	0.25 -1.5	2 -7	3-7	-	17-37	120-1080	-	-	-		-	1-7 (FC) ppm	-	[1]
As (III), As (V)	Botryococcus Braunii	-	50-2000	2-12	-	-	240-21600	-	-	-	5-90	-	-	-	[2]
As(III) and As(V)	Rice polish	0.001-0.0014	0.2-1	3-11	-	25	-	-	-	-	-	0.0001-0.03	-	-	[3]
As(III)	Leucaena leucocephala seed powder	2-6	0.05-50	2-10	-	-	10 - 60	-	-	-	-	-	-	-	[4]
As (V)	Iron oxide modified rice husk char	2.5-50	0.05-10	2-12	-	-	15-1440	-	-	-	82-96	-	-	-	[5]
As (V)	Activated Opuntia ficus	-	-	-	-	-	-	-	-	-	-	-	-	-	[6]

	biomass char														
Cd (II)	Bacillus Subtilis	1-4	25-500	3-8	-	25	20-240	-	-	-	-	-	-	-	[7]
Cd (II)	Shells of B. bengalensis	2-10	25-1000	2-7	-	-	10-80	-	-	-	-	-	-	-	[8]
Cd (II)	Spirulina (Arthrospira) spp	0.1	1-10	6-8	12-16	-	0-1500	-	-	-	50-80	-	-	-	[9]
Cd(II)	Valonia resin	1	10-150	2-7	-	20-90	0-180	-	-	-	-	-	-	-	[10]
Cd(II)	Gossypium barbadense waste	2.5-40	25-800	2-10	-	-	5-150	0.125 - 1	-	-	2-100	-	-	-	[11]
Cd(II)	Alkali modified oak waste residues	0.05-10	25-100	2-8	-	10-40	5-240	-	-	-	26-99.5	-	-	-	[12]
Cd(II)	Moringa Oleifera Seed Powder	2-6	0.01-0.1	4.5-8.5	-	-	10-60	-	-	-	-	-	-	-	[13]
Cd(II)	Rice straw	0.1-0.5	10-100	2-7	-	-	-	-	-	-	-	-	-	-	[14]
Cd(II)	Jackfruit mango and rubber leaves	0.2 -10	10 -100	2-8	-	-	5-180	-	-	-	36.62 - 99.71	-	-	-	[15]
Co(II)	Alginate-SBA-15 nanocomposite	-	5-250	2-7	-	-	60-300	-	-	-	-	2-80	-	-	[16]

Cr (VI)	Chitosan oligosaccharide-coated iron oxide nanoparticles	0.1-1	10-35	2-10	-	28-38	10-60	-	-	-	20-100	-	-	-	[17]
Cr(VI)	Cyanobacterial biomass	0.5-2.5	2.5-25	5-11	-	25-45	0-5	-	-	-	10-100	-	-	-	[18]
Cr(VI)	Date-palm-leaves and broad-bean-shoots	1-6	20 -140	1-10	-	-	20-180	-	-	-	-	-	-	-	[19]
Cr(VI)	Borasus Flabellifer Coir Powder	0.1-0.7	5-30	1-10	-	30-50	0-120	0.063-0.125	-	-	-	-	-	-	[20]
Cr(VI)	Borasus Flabellifer coir powder and ragi husk powder	0.1-1	20-100	1-7	-	-	0-120	0.063-0.125	-	-	-	-	-	-	[21]
Cr(VI), Cr(III)	Nanocrystalline cellulose (NCC)	0.5 -4	0.5-50	2.5-8.5	-	-	10-60	-	-	-	5-100	-	-	-	[22]
Cr(VI)	Jackfruit leaf, mango leaf, onion peel, garlic peel, bamboo leaf, acid treated rubber leaf and coconut shell powder	0.5-10	10-100	1-7	-	30-50	5-270	-	-	-	4.32-100	-	-	-	[23]

Cr(VI)	Date palm fiber	0.1-4(%w/v)	181-419	3.2-6.8	-	-	5-60	-	-	-	-	-	-	-	[24]
Cr(VI)	Iron doped rice husk	2.5-10	25-100	2-6	-	20-50	0-240	-	-	-	30-100	-	-	-	[25]
Cr (VI)	Coconut shell, neem leaves, hyacinth roots, rice husk, rice bran, rice straw, neem bark, and sawdust	2.5-30	3-300	1-11	-	-	0-420	-	-	-	10-100	-	-	-	[26]
Cr(VI)	Maize bran	-	200-300	2-8.5	-	-	10-180	-	-	-	-	2-12	-	-	[27]
Cr (VI)	Pongamia cake	1-3	75-500	2-7	-	30	-	-	-	20-160	-	-	-	-	[28]
Cr (VI)	Agriculture waste carbon	1-10	2-80	2-6	-	-	5-180	-	-	-	20-100	-	-	-	[29]
Cr (VI)	Medler seed based activated carbon	0.5-3	50-200	1-6	-	30-60	400-750	-	-	-	20-100	-	-	-	[30]
Cr (VI)	Sawdust based nanocomposite	-	-	-	-	-	-	-	-	-	-	0.1-700	-	-	[31]
Cu (II)	Date palm seeds	0.05-0.5	5-100	2-6	-	-	-	-	-	-	-	-	-	-	[32]

Cu (II)	Gundelia tournefortii	0.1-2	10-200	2-7	-	20-40	2-120	-	-	-	-	0.1-40	-	-	[33]
Cu (II)	Carboxylated cellulose nanowhiskers	0.2-10	10-60	4-10	-	6-25	-	-	-	-	25-100	-	-	-	[34]
Cu (II)	Banana flower	-	10-100	3.2-5.6	250-400	-	0-160	0.17 – 0.06	-	-	-	2.5-25	-	-	[35]
Cu (II)	Sawdust	-	50-80	3-6	-	25-40	-	0.050-0.2	-	-	60-90	-	-	-	[36]
Cu (II)	Flax meal	1-10	20-200	2-5	200-300	20-40	-	-	-	-	-	0.1-35	-	-	[37]
Cu (II)	Pumice	0.2-2	-	2-10	-	30-60	5-120	-	-	-	-	-	-	-	[38]
Cu (II)	Rambutan (Nephelium lappaceum) peel	0.04-0.4	-	-	-	-	-	-	-	-	-	-	-	-	[39]
Cu (II)	Acid modified coconut husk char	0.1-1	10-60	1-12	-	-	10-100	-	-	-	45-100	-	-	-	[40]
Cu (II)+dye	Sawdust	-	-	-	-	-	-	-	-	-	-	-	-	-	[41]
Hg (II)	Sargassum Bevanom algae	0.1-0.45	50-200	1-10	-	20-50	10-90	-	-	20-100	-	-	-	-	[42]
Hg (II)	Yeast Yarrowia lipolytica	-	20-60	4-8		15-35	360-1080	-	-		-	-	-	-	[43]

Hg (II)	Walnut shell biochar	-	10-80 ppm 1000 - 300(S)	2-11	-	25-45	0-120	-	-	10-100	-	-	-	-	[44]
Pb (II)	Thiosemicarbazide modified chitosan	-	10-60	-	-	25-55	-	-	-	-	70-95	-	-	-6 - -1 Kj/mol	[45]
Pb (II)	Hydroxyapatite/chitosan nanocomposite	0.01-1	20-5000	2-6	80-400	25-55	15-360	-	-	10-75%	-	-	-	-	[46]
Pb(II)	Antep pistachio shells	0.5-4	5-100	2-9.5	-	30-60	5-120	-	-	-	26.4 - 98.7	-	-	-	[47]
Pb (II)	Rice straw nanocellulose fibers	0.1-1	1-50	2-8.5	-	10-60	-	-	-	100-300	-	-	-	-	[48]
Pb (II)	Olive stone	-	50-250	3-5	-	-	-	-	-	-	-	-	-	-	[49]
Pb (II)	Carboxylate-functionalized walnut shell (CFWS	0.2-1	100-220	-	-	-	0-20	-	-	-	30-90	-	-	-	[50]
Pb (II)	Gundelia tournefortii.	.01-0.12	5-100	-	-	20-50	5-60	-	-	-	-	2-120	-	-	[51]
Pb (II)	Black cumin	0.1-0.5	-	2-6	-	20-50	-	-	-	-	-	1-8	-	-	[52]
Pb (II)	Iron oxide nanocomposites from bio-waste mass	0.1-0.8	10-100	3-4	-	-	20-120	-	-	-	20-80	-	-	-	[53]

Pb (II)	Rice husk char	0.1	25	-	-	400-800	0-120	-	-	-	2-100	0.2-6	-	-	[54]
Pb (II)	Rice husk carbon	1-10	20-80	-	-	-	5-180	-	-	-	20-100	-	-	-	[55]
Ni (II)	Alginate-based composite beads	0.5-3	100-300	1-10	-	-	-	-	-	-	-	-	-	-	[56]
Ni (II)	Potamogeton pectinatus	2.5-60	5-300	2-8	-	-	5-180	0.125–0.25	-	-	-	-	-	-	[57]
Ni (II)	Sugarcane bagasse, passion fruit waste, orange peel and pineapple peel, and commercial activated carbon	-	50-300	4.6-6	-	-	0-360	0.25 - 0.5	0.75 – 65.2	-	-	-	-	-	[41]
Th (IV)	Chitosan/TiO2 nanocomposite	0.1-0.25	-	3-8	-	25-45	30-80	-	-	-	-	-	-	-	[58]
U (VI)	Polyacrylonitrile-grafted potato starch based resin	0.05-0.5	8.4-150		-	-	5-180	-	-	-	30-100	-	2-7 pH	-	[59]
Ur (VI)	KMnO4 modified hazel nut	0.5-8	25-250	2-7	-	293K-318K	20-200	-	-	-	6-75	-		-	[60]

	shell biochar														
Zn(II)	Peanut shells	0.05-0.5	5-50	3-7	-	25-45	0-60	-	-	-	2-35	-	-	-	[61]
Zn(II)	Pongamia cake	1-5	50-500	2-7	-	30-50	-	-	-	-	-	28-100	-	-	[62]
Zn (II)	Hazelnut Shell	2-10	25	2-8	-	30-60	10-120	-	-	-	-	-	-	-	[38]
Zn (II)	Rice husk biochar	-	-	-	-	400-600	15-120	-	-	-	-	5.66-5.76	-	-	[63]
Ni (II)	Alginate nanoparticles	5-15	-	2-6	-		5-80	-	-	-	10-100	-	-	-	[64]
Co (II)		2-6	-		-			-	-	-	-	-	-	-	
Co (II) Ni (II)	Carboxymethyl chitosan-bounded Fe3O4 nanoparticles	0.03-0.12	43-157	4-8	-	-	20-60	-	-	-	-	5.84-80.33	-	-	[65]
Cu (II), Pb (II)	Rice straw and Fe_3O_4 nanoparticles	0.1-0.15	30 -170		-	-	10-110	-	-	-	-		-	-	[66]
Ni (II), Cd (II)	Typha domingensis	2.5-40	25-300	2-8	-	-	5-150	0.25-1	-	-	-	-	-	-	[67]
Cd (II) Zn (II)	Sargassum filipendula	-	6 -13 mequiv/L	-	-	-	-	-	-	-	-	-	-	-	[68]
Cu(II) and Cr(VI)	Wheat straw	-	-	2-5	-	25-60	10-20	0.25-0.85	-	-		0.1-3	-	-	[69]

Cd (II), Pb(II), Ni (II)	Itaconic acid grafted poly (vinyl) alcohol encapsulated wood pulp	0.08-0.36	5-50	-	-	25-45	20-50	-	-	-	86-99	-	-	-	[70]
Pb (II), Cd(II), Ni(II) and Zn(II)	Jacaranda fruit, plum kernels and nutshell	-	20-250	-	-	-	-	-	-	-	-	1-4	-	-	[71]
Cd(II), Pb(II), and Ni(II)	Chicken Feathers	-	0.1-3 mmol/L	3-5	-	-	-	-	-	-	-	0.001-0.03 mmol/g	-	-	[72]
Cd(II), Al (III) Co (II),Cu(II), Fe (II) and Pb (II)	Chitosan and Chitosan—Montmorillonite Nanocomposite	0.2-0.8	-	3-8		-	60-80	-	-	-	15-90	-	-	-	[73]

Table S2. . Range of experimental input and output adsorption variables used in modelling column based- biomaterial adsorption system (AD: Adsorbent dose, IC: Initial concentration, BD: Bed depth, FR: Flow rate, EFR: Effluent flow rate, EC: Effluent concentration, η : % removal or adsorption efficiency, AC : Adsorption capacity)

Metal adsorbed	Biomaterials	AD	IC	pH	BD	FR	EFR	CT	EC	PS	η	MAC	References
		g	mg/L		cm	mL/min	mL/min	min	mg/L	mm		mg/g	

As(III) As(V)	Rice polish	-	0.001-1	-	5-25	1-9	-	-	-	-	-	0.002-0.041	[3]
Cd (II)	Jackfruit, mango and rubber leaves	1.5-4.5	20-80	6	3-9	10-25	-	-	-	-	1-100	-	[15]
Cr(VI)	Alginate immobilized Sargassum sp	3-9	25-117	-	5-14	3.3-6.6	-	-	-	-	65-95	-	[74]
Cr(VI)	Mango, jackfruit, and rubber leaves	-	4.6-81.4	1.5-2	3-9	5-25	-	5-1020	-	-	1-100	-	[23]
Cr(VI)	Peanut shell and almond shell	-	10-20	1-2	-	10-22	-	0-1410	0-19.51	-	2.47-100	-	[75]
Cr (VI)	Pongamia cake	-	75-500		4-12	5-10	-	-	-	-	-	20-150	[28]
Co(II)	Sunflower shells	1.27-3.8	20-60	3-5	5-15	8-19	-	0-150	-	0.25- 2	-	-	[76]
Cu (II)	Shells of sunflower	-	20-60	3-5.6	5-15	9-21	-	-	-	0.25- 2	-	-	[76]
Cu (II)	Walnut shell	-	10-20	-	5-10	-	-	0-1140	0-20	-	-	-	[77]
Ni (II)	Alginate-based composite beads	3-9	100-300	-	-	2-6	-	-	-	-	-	-	[56]
Ur (VI)	Zinc oxide nanoparticles–chitosan	0.2-0.4	0.5-2.5	7.5-11.5		2-6	1-3	-	8.5-84	-	-	-	[78]
Zn(II)	Pongamia cake	-	50-500	-	4-12	5-15	-	-	-	-	-	25-70	[62]

Cr (VI), Zn (II), Cr (II)	Chitosan foamed structure	-	-	-	-	-	-	-	-	-	-	2-80	[79]

S3. Surface morphology of biomaterials under scanning electron microscopy

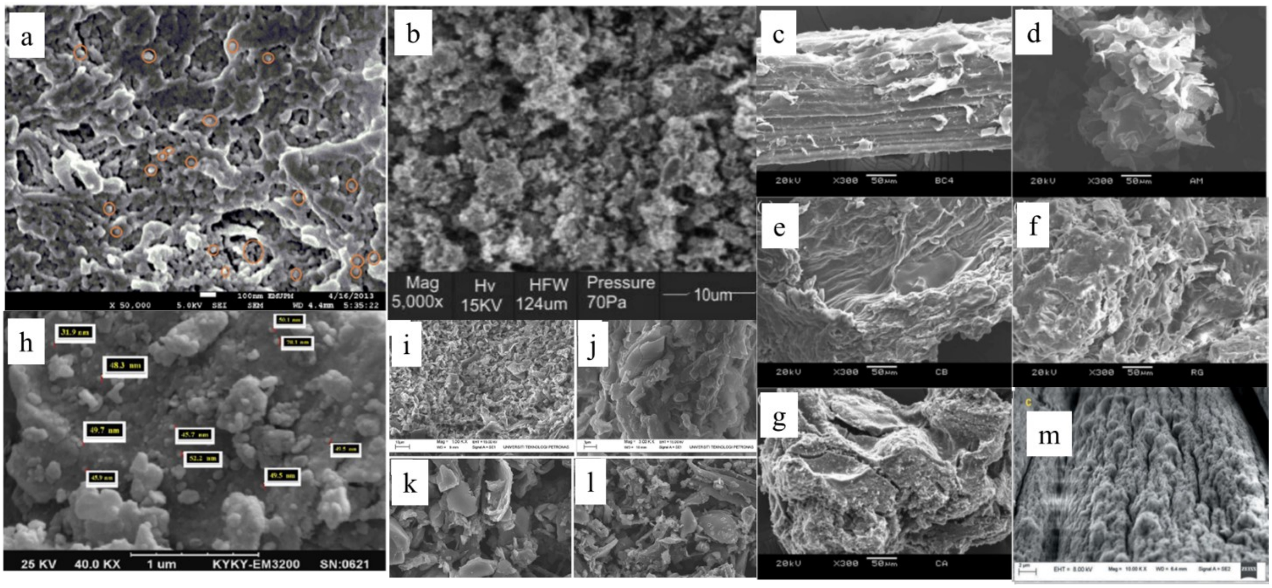

Fig. S2. SEM images of some biomaterials reviewed in this study [41,54,64,74,78,80]

(a) Zinc oxide nanoparticles-chitosan; (b) Nano magnetite coated walnut-rice husk ; (c) Sugarcane bagasse, (d) Passion fruit waste, (e) Orange peel, (f) Pineapple peel and (g) Carbonaceous material, (h) Alginate nanoparticles, (i), (j), (k) and (l) treated rice husk at 400 ^{o}C, m) treated alginate-immobilized Sargassum sp.

S4. Frequency of independent adsorption variables that are used as input parameters in ANN-frameworks

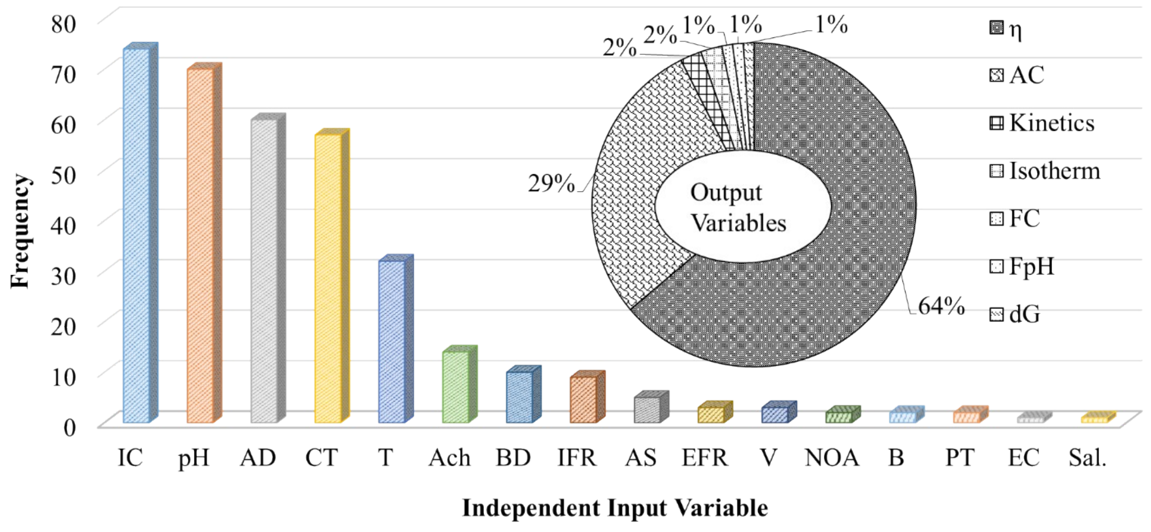

Fig.S3. Frequency of independent adsorption variables that are used as input parameters in ANN-frameworks

S5 Standalone ANN Scheme

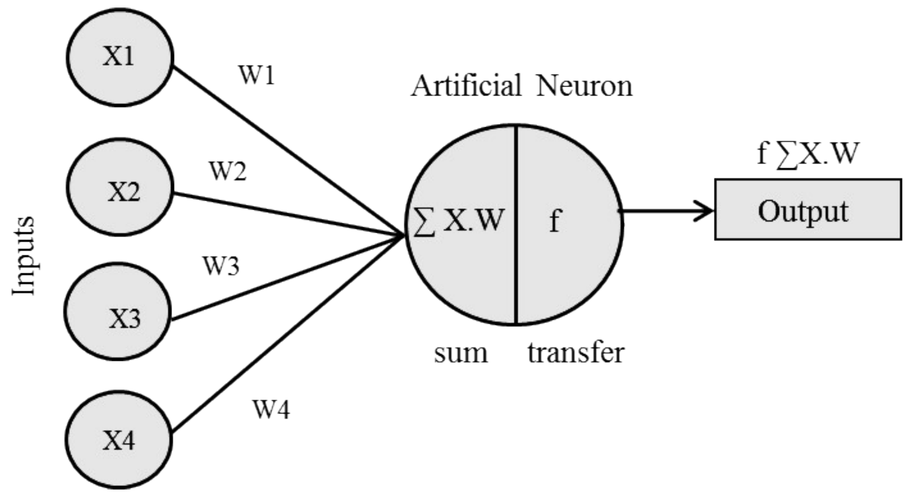

Fig.S4. General ANN Scheme

Fig. S4 Details of activation function used in the reviewed literature

S5.1 Details of activation function

Table S3. List of activation functions commonly used in the literature for modelling metal ion sorption onto biomaterials.

Activation function	Representation	Equation *
Hyperbolic Tangent	$tansig(x)$	$\frac{2}{(1+\exp(-2x))} - 1$
Pure Linear	$purelin(x)$	x
Log sigmoid	$logsig(x)$	$\log \frac{1}{(1+\exp(-x))}$
Sigmoid	*Sig (x)*	$\frac{1}{(1+\exp(-x))}$

$*\ (x)$ denotes dependent variable. Data depicted using information acquired from [81].

S5.2 Numerical representations of ANN models

- The output of ANN at a particular node k can be presented in the mathematical form as an equation

$$y_k = \varphi\left(\sum_{j=1}^{m} W_{kj}.x_j + b_k\right) \tag{1}$$

where y_k is the output at node k, φ is the transfer function, W_{kj} is the weight connecting node

k from node j, x_j = input values from node j, b_k is the bias added to node k.

- The iterative process for weight adjustments using the backpropagation algorithm can be formulated mathematically :

$$w^{k+1}_{ij} = w^{k}_{ij} + \eta\, \delta^{k}_{j} I_i f'(s) \tag{2}$$

- The error function is given by :

$$E = \sum_{n=1}^{N} (O_n - O_d)^2$$
(3)

S5.3 Mathematical formulations commonly used statistical parameters

$$R^2 = 1 - \frac{\sum_{i=1}^{N} (y_{m,i} - y_{e,i})^2}{\sum_{i=1}^{N} (y_{m,i} - y_{e\ av})^2}$$
(4)

$$R = \frac{\sum_{i=1}^{n} \left[(y_{m,i} - y_{m,av}) * (y_{e,i} - y_{e,,av}) \right]}{\sqrt{\sum_{i=1}^{n} \left[(y_{m,i} - y_{m,av})^2 \right] * \sum_{i=1}^{n} (y_{e,i} - y_{e,av})}}$$
(5)

$$MSE = \frac{1}{N} \sum_{i=1}^{N} (y_{m,i} - y_{e,i})^2$$
(6)

$$RMSE = \sqrt{\frac{\sum_{i=1}^{n} (y_{m,i} - y_{e,i})^2}{n}}$$
(7)

* y_m :predicted value, y_e :experimental value

S5.4 Feedforward neural network applied to model sorption of metal ion on biomaterial-based adsorption system

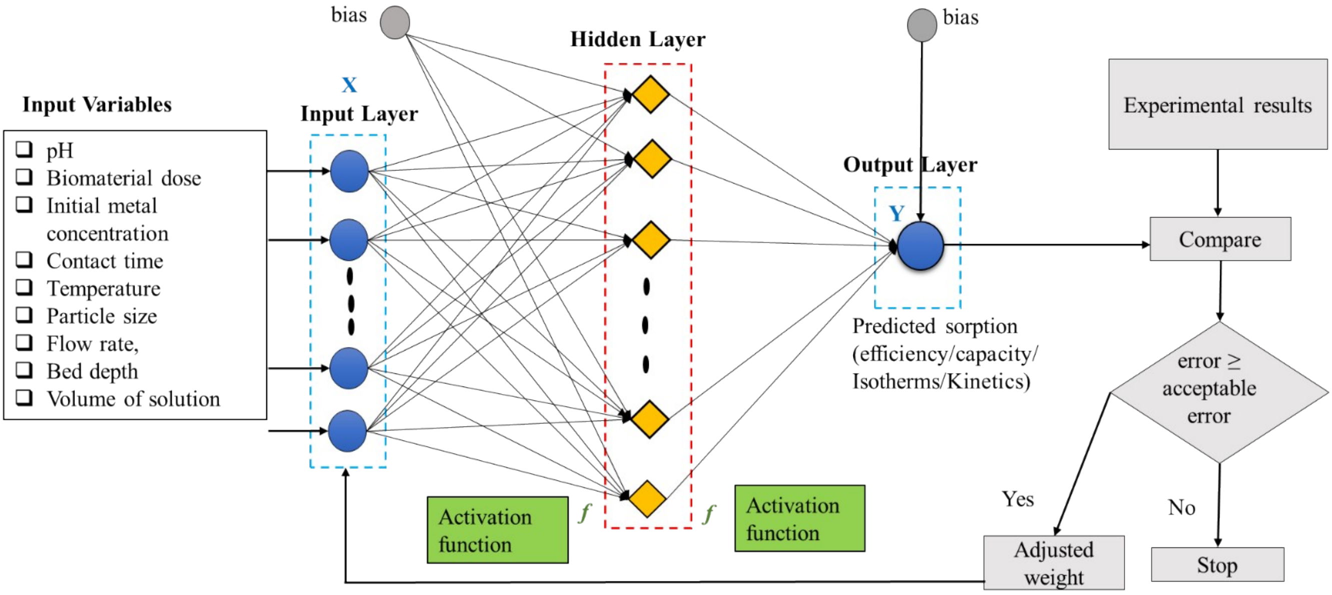

Fig.S5 Schematic of FFNNs applied to simulate metal adsorption process

S5.5 Details of input and output parameters of standalone frameworks for optimizing metal adsorption process

Table S4. Details of the parameters considered at the input and output layer of ANN. (AD: Adsorbent dose, IC: Initial concentration, BD: Bed depth, FR: Flow rate, EFR: Effluent flow rate, EC: Effluent concentration, NOA : no. of adsorbent, η : % removal or adsorption efficiency, AC : Adsorption capacity,G= Gibbs free energy changes)

Metals	Biomaterials	Data at the Input Layer														At the output layer				Ref.
		AD	CT	IC	pH	T	AS	B	BD	FR	EFR /EC	VS	HAp	Ach	NOA	η	AC	FC	dG	
As(III) As(V)	Rice polish	1		1	1	1	-	-	1	1	-	-	-	-	-	-	1	-	-	[3]
As (III)	Leucaena leucocephala Seed powder	1	1	1	1	-	-	-	-	-	-	-	-	-	-	1	-	-	-	[4]
As (V)	Iron oxide modified rice husk char	1	1	1	1	-	-	-	-	-	-	-	-	-	-	1	-	-	-	[5]
As (V)	Activated Opuntia ficus biomass char	-	1	1	1	1	-	-	-	-	-	-	-	-	-	-		-	-	[6]
Cd (II)	Valonia resin	-	1	1	1	1	-	-	-	-	-	-	-	1	-	-	1	-	-	[10]
Cd (II)	Gossypium barbadense waste	1	1	1	1	-	-	-	-	-	-	-	-	1	-	-	1	-	-	[11]
Cd (II)	Alkali modified oak waste residues	1	1	1	-	1	-	-	-	-	-	-	-	-	-	1	-	-	-	[12]
Cd (II)	Moringa Oleifera Seed	-	-	1	1	1	-	-	-	-	-	-	-	1	-	1	-	-	-	[13]

	Powder																			
Cd (II)	Rice straw	1	-	1	1	-	-	-	-	-	-	-	-	-	-	1	-	-	-	[14]
Cd (II)	Jackfruit, mango and rubber leaves	-	1	-	-	-	-	-	1	1	1	-	-	-	1	1	-	-	-	[15]
Cr(VI)	Date-palm-leaves (DPL) and broad-bean-shoots (BBS)	1	1	1	1	-	-	-	-	-	-	-	-	-	-	1	-	-	-	[19]
Cr(VI)	Borasus Flabellifer Coir Powder	1	-	1	1	-	-	-	-	-	-	-	-	-	-	1	-	-	-	(Krishna & Sree, 2014)
Cr(VI)	Borasus Flabellifer coir powder and Ragi Husk powder	1	-	1	1	-	-	-	-	-	-	-	-	-	-	1	-	-	-	[21]
Cr(VI)	Mango, jackfruit, and rubber leaves	-	1	-	1	-	-	-	1	1	-	-	-	-	1	-	-	-	-	[23]
Cr(VI)	Date palm fiber	1	1	1	1	-	-	-	-	-	-	-	-	-	-	1	-	-	-	[24]
Cr(VI)	Peanut shell and almond shell	-	-	1	1	1	-	-	1	1	1	-	-	-	-	-	1	-	-	[75]

Cr(VI)	Iron doped rice husk	1	1	-	1	1	1	-	-	-	-	-	-	-	-	1	-	-	-	[25]
Cr(VI)	Maize bran		1	1	1	1	-	-	-	-	-	-	-	-	-	-	1	-	-	[27]
Cr (VI)	Pongamia oil cake	-	-	1	-	-	-	1	1	-	-	-	-	-	-	-	1	-	-	[28]
Cr (VI)	Chitosan Oligosaccharide-coated iron oxide nanoparticles	1	1	1	1	1	-	-	-	-	-	-	-	-	-	1	-	-	-	[17]
Cr(VI)	Alginate immobilized Sargassum sp	-	-	1	-	-	-	-	1	1	-	-	-	-	-	1	-	-	-	[74]
Cr (VI)	Medler seed based activated carbon	1	1	1	1	1	-	-	-	-	-	-	-	-	-	1	-	-	-	[30]
Cr (VI)	Sawdust based nanocomposite	1	1	1	1	1	-	-	-	-	-	-	-	-	-	-	1	-	-	[31]
Co(II)	Alginate-SBA-15 nanocomposite	-	1	1	1	1	-	-	-	-	-	-	-	-	-	1	-	-	-	[16]
Co(II)	Sunflower biomass	1	-	1	1	-	-	-	1	1	-	-	-	1	-	1	-	-	-	[76]
Cu (II)	Shells of sunflower	1	-	1	1	-	-	-	1	1	-	-	-	1	-	1	-	-	-	[82]

Cu (II)	Date palm seeds	1	-	1	1	-	-	-	-	-	-	-	-	-	-	-	1	-	-	[32]
Cu (II)	Gundelia tournefortii	1	1	1	1	1	-	-	-	-	-	-	-	-	-	-	1	-	-	[33]
Cu (II)	Carboxylated cellulose nanowhiskers	1	-	1	-	-	1	-	-	-	-	-	-	-	-	1	-	-	-	[34]
Cu (II)	Banana flower	-	1	-	1	-	1	-	-	-	-	-	-	1	-	1	-	-	-	[35]
Cu (II)	Sawdust of mango tree (Mangifera indica)	-	-	1	1	1	-	-	-	-	-	-	-	1	-	1	-	-	-	[36]
Cu (II)	Walnut shell	-	1	1	1	-	-	-	1	-	1	-	-	-	-	1	-	-	-	[83]
Cu (II)	Flax meal	1	-	1	1	-	-	-	-	-	-	-	-	-	-		1	-	-	[37]
Cu (II)	Acid modified coconut husk char	1	1	1	1	-	-	-	-	-	-	-	-	-	-	1	-	-	-	[40]
Cu (II)	Rambutan Peel	1	1	1	-	1	-	-	-	-	-	-	-	-	-	-	-	1	-	[39]
Pb (II)	Thiosemicarbazide modified chitosan	-	-	1	-	1	-	-	-	-	-	-	-	-	-	1	-	-	1	[45]

Pb (II)	Hydroxyapatite/chitosan Nanocomposite	1	1	1	1	-	1	-	-	-	-	-	1	-	-	-	1	-	-	[46]
Pb (II)	Rice husk char	1	1	1	1	-	-	-	-	-	-	-	-	-	-	1	-	-	-	[84]
Pb(II)	Antep pistachio shells	1	1	1	1	1	-	-	-	-	-	-	-	-	-	1	-	-	-	[47]
Pb (II)	Rice straw nanocellulose fibers	1	1	1	1	-	-	-	-	-	-	1	-	-	-	1	-	-	-	[48]
Pb (II)	Olive stone	1		1	1	-	-	-	-	-	-	-	-	-	-	-	-	-	-	[49]
Pb (II)	Carboxylate-functionalized walnut shell (CFWS	1	1	1	1	-	-	-	-	-	-	-	-	-	-	1	-	-	-	[50]
Pb (II)	Gundelia tournefortii.	1	1	1	1	-	-	-	-	-	-	-	-	-	-	-	1	-	-	[51]
Pb (II)	Black cumin	1	-	-	1	1	-	-	-	-	-	-	-	-	-	-	1	-	-	[52]
Pb (II)	Iron oxide nanocomposites from bio-waste mass	1	1	1	1	-	-	-	-	-	-	-	-	-	-	1	-	-	-	[53]

Ni (II)	Alginate-based composite beads	-	1	1	1	1	-	-	-	-	-	-	-	-	-	1	1	-	-	[56]
Ni (II)	Potamogeton pectinatus	1	1	1	1	-	-	-	-	-	-	-	-	1	-	1	-	-	-	[57]
Ni (II)	Sugarcane bagasse, passion fruit waste, orange Peel and pineapple peel, and commercial activated carbon	-	1	1	1	-	-	-	-	-	-	-	-	1	-	-	1	-	-	[41]
Zn (II)	Rice husk biochar		1	1		1	-	-	-	-	-	-	-	-	-		1	-	-	[63]
Zn(II)	Peanut shells	1	-	1	1	-	-	-	-	-	-	-	-	-	-	-	1	-	-	[61]
Zn(II)	Pongamia oil cake	1	-	1	1	1	-	-	1	1	-	-	-	-	-	-	1`	-	-	[62]
Zn (II)	Hazelnut Shell	1	1	-	1	1	-	-	-	-	-	-	-	-	-	-	1	-	-	[38]

Hg (II)	Walnut shell biochar		1	1	1	1	-	-	-	-	-	-	Salinity -1	-	-	1	-	-	-	[44]
Ur (VI)	$KMnO_4$ modified hazel nut shell biochar	1	1	1	1	1	-	-	-	-	-	-	-	-	-	1	-	-	-	[60]
Ur (VI)	Zinc oxide nanoparticles –chitosan	1	-	-	1	-	-	-	-	1	1	1	1	-	-	1	-	-	-	[78]
Th (IV)	Chitosan /TiO_2 nanocomposite	1	1	-	1	-	-	-	-	-	-	-	-	-	-	-	1	-	-	[58]
U (VI)	Polyacrylonitrile-grafted potato starch based resin	1	1	1	1	1	-	-	-	-	-	-	-	-	-	1	-	-	1	[59]
Cr(VI) Cr(III)	Nanocrystalline cellulose (NCC)	1		1	1	-	-	-	-	-	-	-	-	-	-	1	-	-	-	[22]

Pb (II), Co (II)	Rafsanjan pistachio shell	1	-	1	1	1	-	-	-	-	-	-	-	-	-	-	1	-	-	[85]
Cu (II), Pb (II)	Rice straw and Fe_3O_4 nanoparticles	1	1	1	-	-	-	-	-	-	-	-	-	-	-	1	-	-	-	[66]
Ni (II), Cd (II)	Typha domingensis	1	1	1	1	-	-	-	-	-	-	-	-	1	-	1	-	-	-	[67]
Cu(II) Cr(VI)	Wheat straw	-	1	1	1	-	-	-	-	-	-	-	-	1	-	-	1	-	-	[69]
Cd (II), Pb(II), Ni (II)	Itaconic acid grafted poly (vinyl) alcohol encapsulated wood pulp (IA-g-PVA-en-WP)	1	1	1	-	-	-	-	-	-	-	-	-	-	-	-	1	-	-	[70]
Pb (II) Cd (II) , Ni (II) and Zn (II)	Jacaranda fruit, plum kernels and nutshell	-	1	1	-	-	-	-	-	-	-	-	-		-	-	-	-	-	[86]
Cd(II), Pb(II), and Ni(II)	Chicken Feathers	-	-	1	1	-	-	-	-	-	-	-	-	-	-	1	-	-	-	[72]

Ni (II), Co (II)	Alginate nanoparticles	1	1	-	1	-	-	1	-	-	-	-	-	-	-	1	-	-	-	[64]
Co (II) Ni (II)	Carboxymethyl chitosan-bounded Fe_3O_4 nanoparticles	1	1	1	1	-	-	-	-	-	-	-	-	-	-	1	-	-	-	[65]
Cd(II), Al (III) Co (II),Cu(II), Fe (III) and Pb (II)	Chitosan and Chitosan—Montmorillonite Nanocomposite	1	1	-	1	-	-	-	-	-	-	-	-	-	-	1	-	-	-	[73]-
Cr (VI), Zn (II), Cr (II)	Chitosan foamed structure	-	-	1	-	-	-	-	-	-	-	-	-	-	-	-	1	-	-	[79]
Cr (VI)	Agriculture waste carbon	1	1	1	1	-	-	-	-	-	-	-	-	-	-	-	1	-	-	[29]
Cu (II)+dye	Sawdust	1	1	1	1	-	-	-	-	-	-	-	-	-	-	1	-	-	-	[87]

S5.6. ANN framework for metal adsorption on biomaterials

Table S5. ANN framework for metal adsorption efficiency

Metal adsorbed	Biomaterials	Optimization	TA	Activation Function (IHL-OHL)	ANN Architecture	RMSE	References
As(III) As(V)	Rice polish	ANN RSM	LM	logsig-logsig	4-7-5-1	0.03	[3]
As (III)	Leucaena leucocephala seed powder	ANN	LM	sigmoid- sigmoid	4-14-1	0.004	[4]
Cd (II)	Valonia resin	ANN	RBP	Elliot-logsig	6-25-5-1	0.002	[10]
Cd (II)	Gossypium barbadense waste	ANN	LM	tansig-purelin	5–10–1	$R^2 = 0.923$	[11]
Cd (II)	Alkali modified oak waste residues	ANN	LM	purelin-purelin	5-10-1	R = 0.99	[12]
Cd (II)	Moringa Oleifera Seed Powder	ANN	LM	sigmoid- sigmoid	4-10-1	0.92	[13]
Cd (II)	Rice straw	ANFIS, RSM		tansig-tansig		R = 0.99	[14]
Cd (II)	Jackfruit, mango and rubber leaves	ANN-GA	LM	tansig-tansig		R= 0.97 - 0.99	[15]
Cr(VI)	Mango, jackfruit, and rubber leaves	ANN-GA	LM	-	-	1.47	[23]
Cr(VI)	Peanut shell and almond shell	ANN	LM	tansig-tansig	3-18-1	0.0074	[75]
Cr(VI)	Maize bran	ANN MLR	LM	-	4-10-1	0.15	[27]
Cr (VI)	Pongamia oil cake	ANN RSM	LM	tansig-purelin	4-10-1 (B) 3-7-1 (C)	0.0015	[62]
Cr(VI)	Date-palm-leaves (DPL) and broad-bean-shoots (BBS)	ANFIS MNLR	-	-		0.17	[19]
Cr(VI)	Borasus Flabellifer Coir Powder	ANN-GA	LM	tansig-purelin	3-18-1	$R^2 = 0.99$	[20]
Cr(VI)	Borasus Flabellifer coir powder and Ragi	ANN		sigmoid-linear	3-6-1	0.44	[21]

	Husk powder	BBD					
Cr(VI)	Date palm fiber	ANN	LM	tansig-linear	4-5-1	1.97	[24]
Cr(VI)	Iron doped rice husk	ANN	LM	-	5-10-1	1	[25]
Cr(VI)	Coconut shell, neem leaves, hyacinth roots, rice husk, rice bran, rice straw, neem bark, and sawdust	ANN	LM	Linear-Linear	4-21-1	1.67	[26]
Co(II)	Shells of sunflower	ANN	LM	tansig – purelin	7–5–1	0.014	[76]
Pb (II), Co (II)	Rafsanjan pistachio shell	ANN-GWO	-	-	-	1.1	[85]
Cu(II)	Date palm seeds	ANFIS MLR	-	gaussian-linear	-	0.17	[32]
Cu (II)	Raw gundelia tournefortii	ANN MNLR	LM	tansig-purelin	5-6-1	0.0021	[33]
Cu (II)	Flax meal	ANN RSM	LM	tansig-purelin	3-22-1	0.024	[37]
Cu(II)	Shells of sunflower	ANN	LM	tansig – purelin	7–5–1	0.018	[82]
Cu (II)	Carboxylated cellulose nano-whiskers	ANN RSM	LM	tansig-purelin	3-6-1	1.66	[34]
Cu (II)	Banana flower	ANN-GA				0.634	[35]
Cu (II)	Sawdust of mango tree (Mangifera indica)	ANN	PR	tansig-logsig	4-50-40-27-1	MSE = 0.044	[36]
Cu (II)	Walnut shell	ANN-GA MLR	LM				[83]
Pb (II)	Black cumin seeds	ANN,RSM	LM	tansig – logsig	3-14-1	0.55	[52]
Ni (II)	Sugarcane bagasse, passion fruit waste, orange peel and pineapple peel, and commercial activated carbon	ANN ANFIS	LM	tansig-purelin	4-10-1	R^2 = 0.9943, χ^2 = 0.95 R^2 = 0.9926 , χ^2 = 0.59	[41]
Zn(II)	Peanut shells	ANN	RBP	sigmoid-purelin	3-5-1	R^2 = 0.96	[61]
Zn(II)	Pongamia pinnata)	ANN	LM	tansig-purelin	4-9-1 (B)	0.15	[62]

	Pongamia oil cake	RSM			3-7-1 (C)		
Zn (II)	Hazelnut shells (Corylus pontica)	ANN RSM	LM	tansig - linear	4-8-4	0.003	[38]
Cu(II) and Cr(VI)	Wheat straw	ANFIS		bell shape-linear		(Cu) = 5.9×10^{-3}, (Cr) = 6.0×10^{-3}	[69]
Cd(II), Pb(II), Ni(II)	Itaconic acid grafted poly (vinyl) alcohol encapsulated wood pulp	ANN	LM	sigmoid-sigmoid	4-15-1	(Pb) = 0.184, (Cd) =3.2×10^{-15}, (Ni) = 0.061	[70]
Pb (II)	Hydroxyapatite/chitosan nanocomposite	ANFIS	-	-	-	R= 0.98	[46]
Pb(II)	Antep pistachio shells	ANN	LM	tansig - purelin	5-11-1	0.014	[47]
Pb (II)	Rice straw nanocellulose fibers	ANN	LM	sigmoid-sigmoid	5-10-1	0.007	[48]
Pb (II)	Olive stone	ANFIS				R^2 = 0.95 - 0.99	[49]
Pb (II)	Carboxylate-functionalized walnut shell	ANN MNLR	LM	tansig-linear	4-7-1	R^2 = 0.99	[50]
Pb (II)	Iron oxide nanocomposites from bio-waste mass	ANN	BP	sigmoid-sigmoid	4-7-7-1	0.000076	[53]
Th (IV)	Chitosan/TiO_2 nanocomposite	ANN-GA	LM	tansig-tansig	3-4-1	R^2 =0.99	[58]
Cr (VI), Zn (II), Cu (II)	Chitosan foamed structure	ANN RSM	LM	logsig-logsig		R^2 = 0.94–0.99	[79]
Ni (II)	Alginate-based composite beads	ANN	LM	tansig-tansig	4–10–2	R^2 =0.99	[56]
Ni (II)	Potamogeton pectinatus	ANN RSM	LM	tansig-purelin	5 – 6 – 1	1.18	[57]
U (VI)	Polyacrylonitrile-grafted potato starch based resin	ANN	LM	sigmoid-purelin	5-10 -11-2	rpH = 0.98, r% Ads = 0.97	[59]

S5.7 Details of experimental observations and dataset for ANN development

Table S6. Details of total observation, training, validation and testing subsets for ANN model development

Metal adsorbed	Biomaterials	O	Tr.	Va.	Te.	References
Co(II)	Alginate-SBA-15 nanocomposite	-	-	-	-	[16]
Ni (II)	Alginate-based composite beads	32	19	9	9	[56]
Ni (II), Co (II)	Alginate nanoparticles	-	-	-	-	[64]
Cr(VI)	Alginate immobilized Sargassum sp	9	64	13	13	[74]
Cd (II)	Bacillus Subtilis	90	96	20	13	[1]
As (III)	Bacillus thuringiensis strain WS3	128	137	45	45	[1]
As (III), As (V)	Botryococcus Braunii	227				[2]
Cd (II)	Spirulina (Arthrospira) spp	-	53	12	12	[9]
Cr(VI)	Cyanobacterial biomass	77	-	-	-	[18]
Hg (II)	Sargassum Bevanom algae	31	21	5	5	[42]
Hg (II)	Yeast Yarrowia lipolytica	31	-	-	-	[43]
As (V)	Iron oxide modified rice husk char	30	-	-	-	[5]
Cu (II)	Rambutan (Nephelium lappaceum) peel	480	360		120	[39]
Pb (II)	Rice husk char	46	30	8	8	[54]
Cr (VI)	Agriculture waste carbon	44	30	7	7	[29]
Cu (II)+dye	Sawdust	50	38	6	**6**	[87]
Cr (VI)	Medler seed based activated carbon	59	41	-	18	[30]
Hg (II)	Walnut shell biochar	69	41	14	14	[44]
Ur (VI)	KMnO4 modified hazel nut shell biochar	46	32		14	[60]
Pb (II)	Hydroxyapatite/chitosan nanocomposite	58	38	-	19	[46]
Ur (VI)	Zinc oxide nanoparticles–chitosan	49	35	7	7	[78]
Th (IV)	Chitosan/TiO2 nanocomposite	144	-	-	-	[58]
Co (II)	Carboxymethyl	54	41	-	13	[65]

Ni (II)	chitosan-bounded Fe3O4 nanoparticles					
Cd(II), Al (III) Co (II),Cu(II), Fe (II) and Pb (II)	Chitosan and Chitosan—Montmorillonite Nanocomposite	43	21	11	11	[73]
As(III) and As(V)	Leucaena leucocephala seed powder	31	-	-	-	[4]
As (III)	Valonia resin	180	108	36	36	[10]
Cd (II)	Gossypium barbadense waste	456	366	-	90	[11]
Cd (II)	Moringa Oleifera Seed Powder	219	153	33	33	[13]
Cd (II)	Rice straw	256	244	13	13	[14]
Cd (II)	Jackfruit, mango and rubber leaves	43	30	-	13	[15]
Cr (VI)	Date-palm-leaves (DPL) and broad-bean-shoots (BBS)	93	65	18	10	[19]
Cr(VI)	Borasus Flabellifer coir powder and Ragi Husk powder	54	38	-	16	[21]
Cr(VI)	Mango, jackfruit, and rubber leaves	54	41		13	[23]
(Nag et al., 2020)Cr(VI)	Peanut shell and almond shell	43	32	-	11	[75]
Cr(VI)	Iron doped rice husk	1063	745	212	106	[25]
Cr(VI)	Pongamia oil cake	124	80	18	25	[28]
Co(II)	Rafsanjan pistachio shell	294	149	74	74	[85]
Co (II) Cu (II)	Shells of sunflower	625	500	-	125	[82], [76]
Cu (II)	Date palm seeds	324	162	81	81	[52]
Cu (II)	Gundelia tournefortii	30	-	-	-	[33]
Cu (II)	Banana flower	20	12	4	4	[35]
Cu (II)	Sawdust of mango tree (Mangifera indica)	60	42	9	9	[36]
Cu (II)	Walnut shell	256	244	13	13	[83]
Cu (II)	Antep pistachio shells	528	-	-	-	[47]
Pb(II)	Rice straw nanocellulose fibers	66	34	16	16	[48]
Pb (II)	Gundelia tournefortii.	-	-	-	20	[51]
Pb (II)	Black cumin	83	59	12	12	[52]
Pb (II)	Iron oxide nanocomposites from bio-waste mass	26	15	11	-	[53]
Pb (II)	Potamogeton pectinatus	30	24	6	-	[57]

Ni (II)	Sugarcane bagasse, passion fruit waste, orange peel and pineapple peel, and commercial activated carbon	-	-	-	-	[41]
Ni (II)	Polyacrylonitrile-grafted potato starch based resin	600	420	90	90	[59]
Zn(II)	Pongamia pinnata) Pongamia oil cake	-	-	-	-	[62]
Zn (II)	Hazelnut Shell	100	50	-	50	[38]
Cu (II) Pb (II)	Rice straw and Fe3O4 nanoparticles	-	-	-	-	[66]
Ni (II), Cd (II)	Typha domingensis	-	-	-	-	
Cu(II) and Cr(VI)	Wheat straw	-	-	-	-	[69]
Cd (II), Pb(II), Ni (II)	Itaconic acid grafted poly (vinyl) alcohol encapsulated wood pulp (IA-g-PVA-en-WP)	-	-	-	-	[70]
Pb(II), Cd(II), Ni(II) and Zn(II)	Jacaranda fruit, plum kernels and nutshell	92 - Isotherms 169 - Kinetics				[86]
Cd(II), Pb(II), and Ni(II)	Chicken Feathers	225	157	34	34	[72]

S5.8 Details on learning rate, gradient, momentum, Epoch size and ANN model convergence

Table S7. Information on ANN parameters: learning rate, momentum, max. Epochs, gradient and model convergence

Metal pollutants	Biomaterials	Learning rate	Momentum	Maximum epochs	Minimum gradient	Convergence	Reference
As (V)	Waste Orange Peel	-	-	1000	-	140	[88]
Cd(II)	Gossypium barbadense waste	-	-	6	0.062	6	[11]
Cr(VI)	Jackfruit leaf, mango leaf, onion peel,	-	-	10,000 (GD) 100	-	-	[23]

	garlic peel, bamboo leaf, acid treated rubber leaf and coconut shell powder			(LM)			
Cr(VI)	Iron doped rice husk	-	-	22	-	16	[25]
Cr (VI)	Coconut shell, neem leaves, hyacinth roots, rice husk, rice bran, rice straw, neem bark, and sawdust	0.7	1	32000	-	20,000	[89]
Cu (II)	Sawdust	-	0.7	1000	-	-	[36]
Cu (II)	Flax meal	-	-	450	-	-	[37]
Cu (II)	Pumice	-	-	50	-	-	[38]
Hg (II)	Yeast Yarrowia lipolytica	-	-	10	-	8	[43]
Hg (II)	Walnut shell biochar	-	-	24	-	-	[44]
Pb(II)	Antep pistachio shells	-	-	100	-	12	[47]
Pb (II)	Rice straw nanocellulose fibers	-	0.7	1000	-	-	[48]
Pb (II)	Gundelia tournefortii.	-	-	1000	-	-	[51]
Pb (II)	Black cumin	-	-	3500	0.01	-	[52]
Ni (II)	Potamogeton pectinatus	-	-	6	10.85	6	[57]
Ni (II)	Sugarcane bagasse, passion fruit waste, orange peel and pineapple peel, and commercial	-	-	60 – ANN 250 - ANFIS	10^{-7}	54 167	[41]

	activated carbon						
Th (IV)	Chitosan/TiO 2 nanocomposite	-	-	18	-	12	[58]
Ur (VI)	KMnO4 modified hazel nut shell biochar	-	-	14	-	8	[60]
Zn(II)	Peanut shells	-	-	22	-	16	[61]
Cd (II), Pb(II), Ni (II)	Itaconic acid grafted poly (vinyl) alcohol encapsulated wood pulp (IA-g-PVA-en-WP)	-	-	1500	-	-	[70]
Pb (II), Cd(II), Ni(II) and Zn(II)	Jacaranda fruit, plum kernels and nutshell	-	-	25 (kinetics) 20 (isotherms)	-	23 18	[86]
Cd(II), Pb(II), and Ni(II)	Chicken Feathers	-	-	-	-	-	[72]
Cd(II), Al (III) Co (II),Cu(II), Fe (II) and Pb (II)	Chitosan and Chitosan—Montmorillonite Nanocomposite	-	-	Chitosan 20 CM : 10	-	14 4	[73]
Cr(VI)	Alginate immobilized Sargassum sp	-	-	300 3000	-	ANN-GA : 163 ANN-SA : 2623	[74]
Cr(VI)	Peanut shell and almond shell	-	-	3.2×10^4	-	-	[75]
Ur (VI)	zinc oxide nanoparticles –chitosan	-	-	4	-	2.5	[78]

Zn(II)	Pongamia cake	-	-	6000	-	100	[62]

S5.9 Ensemble ANN framework models

S5.9.1 SOS-ANN working framework

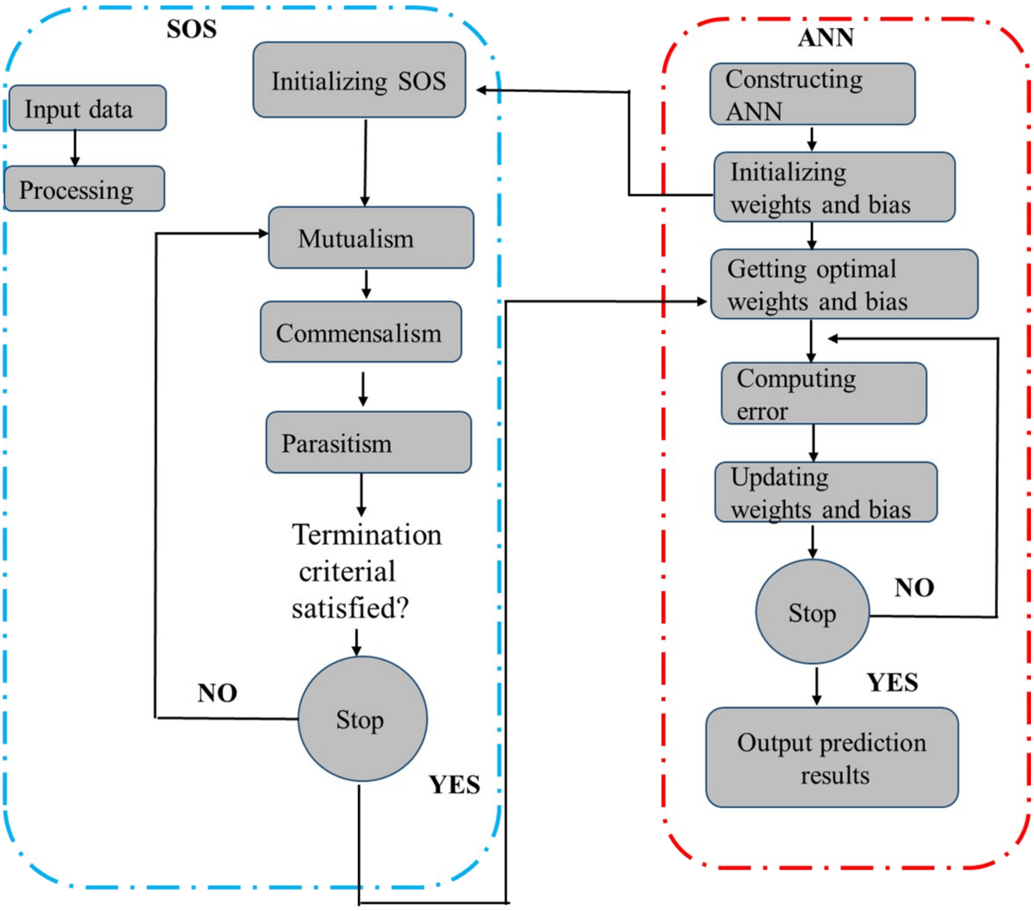

Fig.S6 ANN-SOS Framework

S.5.9.2 GWO-ANN ensemble model

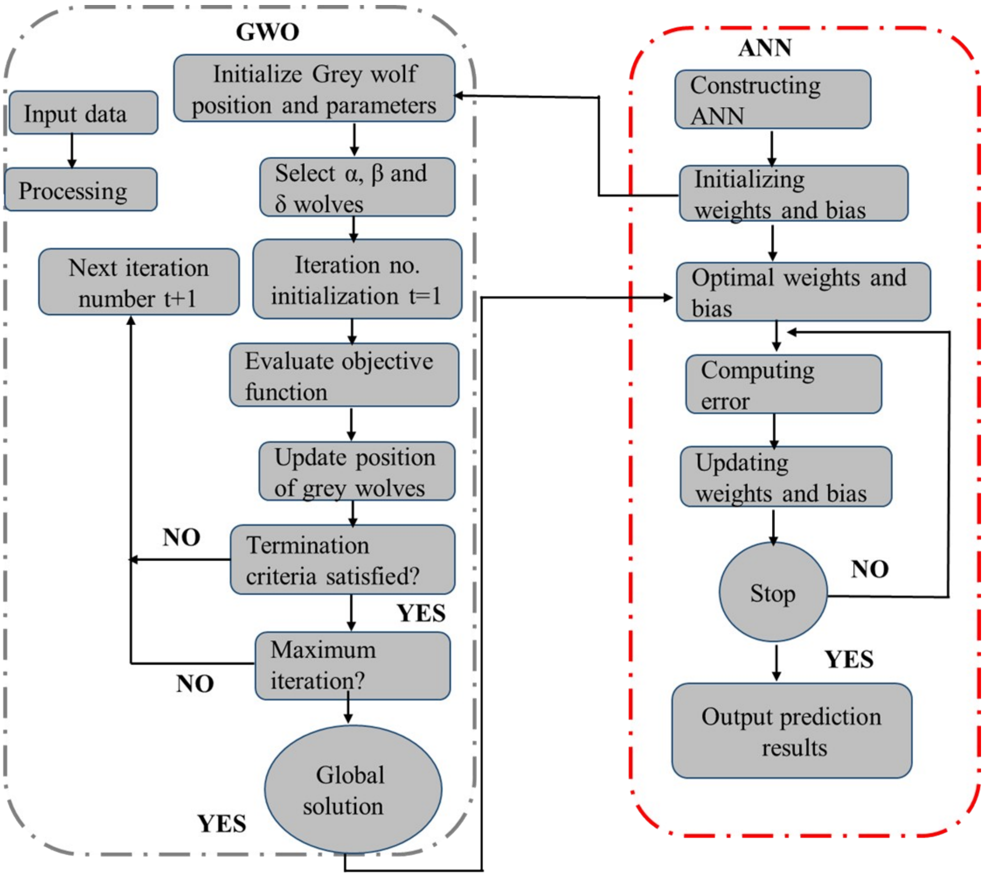

Fig.S7 GWO-ANN framework

S5.9.3 ANFIS

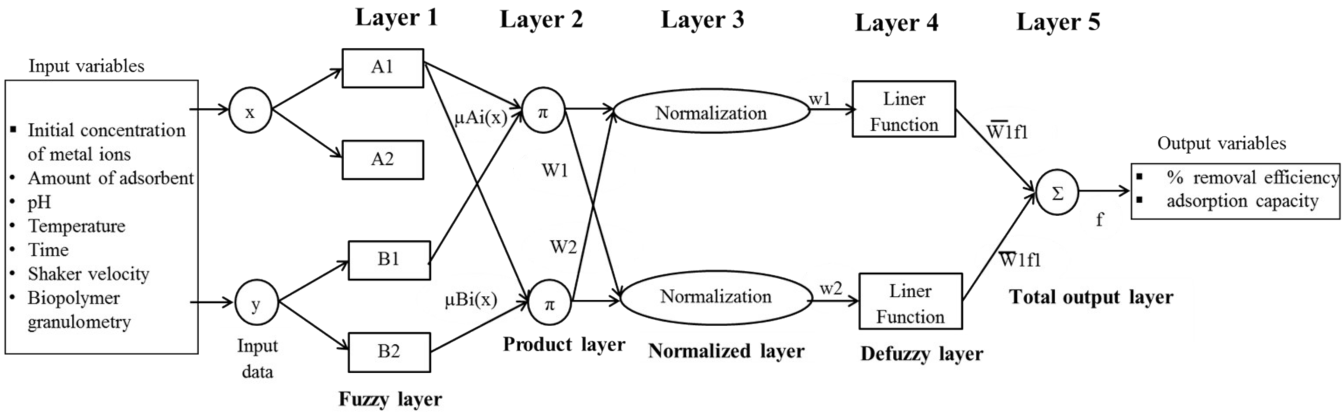

Fig.S8 Schematic of ANFIS structure.

S5.9.3.1 Mathematical formulation of ANFIS layers

Layer 1 $O_1, i = \mu_{Ai}(x), for\ i = 1,2, or\ \ O_1, i = \mu_{Bi} - 2\ (y), for\ i = 3,4$

Membership function: $$\mu_A(x) = \frac{1}{1 + \left|\frac{x - c_i}{a_i}\right|^{2b}}$$

where every i is an adaptive node with a membership function $\mu_A(x)$

Layer 2 $$O_{2,i} = w_i = \mu_{Ai}(x)\mu_{Bi}(y), i = 1,2.$$

where A, B are the premise parameters

Layer 3 $$O_{3,i} = \bar{w}_i = \frac{w_i}{w_1 + w_2} i = 1,2.$$

$\bar{w}_i =$ normalized firing strengths

Layer 4 $$O_{4,i} = \bar{w}_i f_i = \bar{w}_i\ (p_i x + q_i y + r_i)$$

p_i, q_i, r_i = consequent parameters

Layer 5 $$overall\ ouput = O_{5,i} = \sum_i \bar{w}_i f_i = \frac{\sum_i w_i f_i}{\sum_i w_i}$$

S.5.9.4 GA-ANN ensemble model

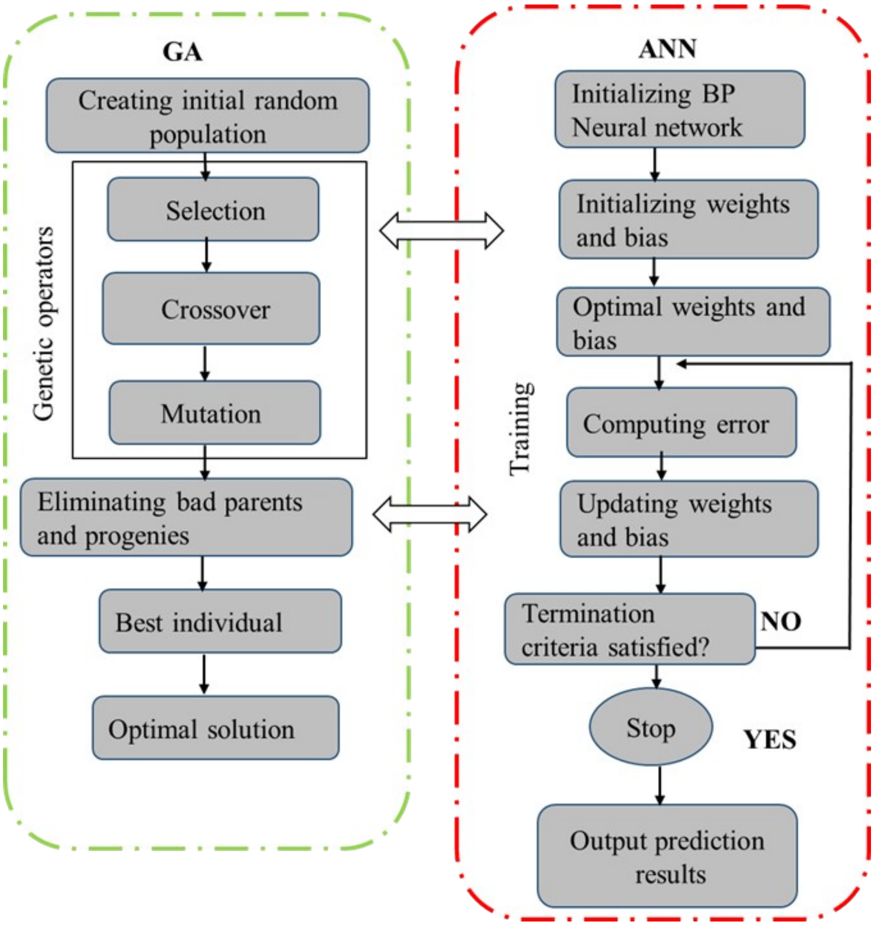

Fig.S9 framework of GA-ANN model

S5.9.5 Queuing search algorithm framework

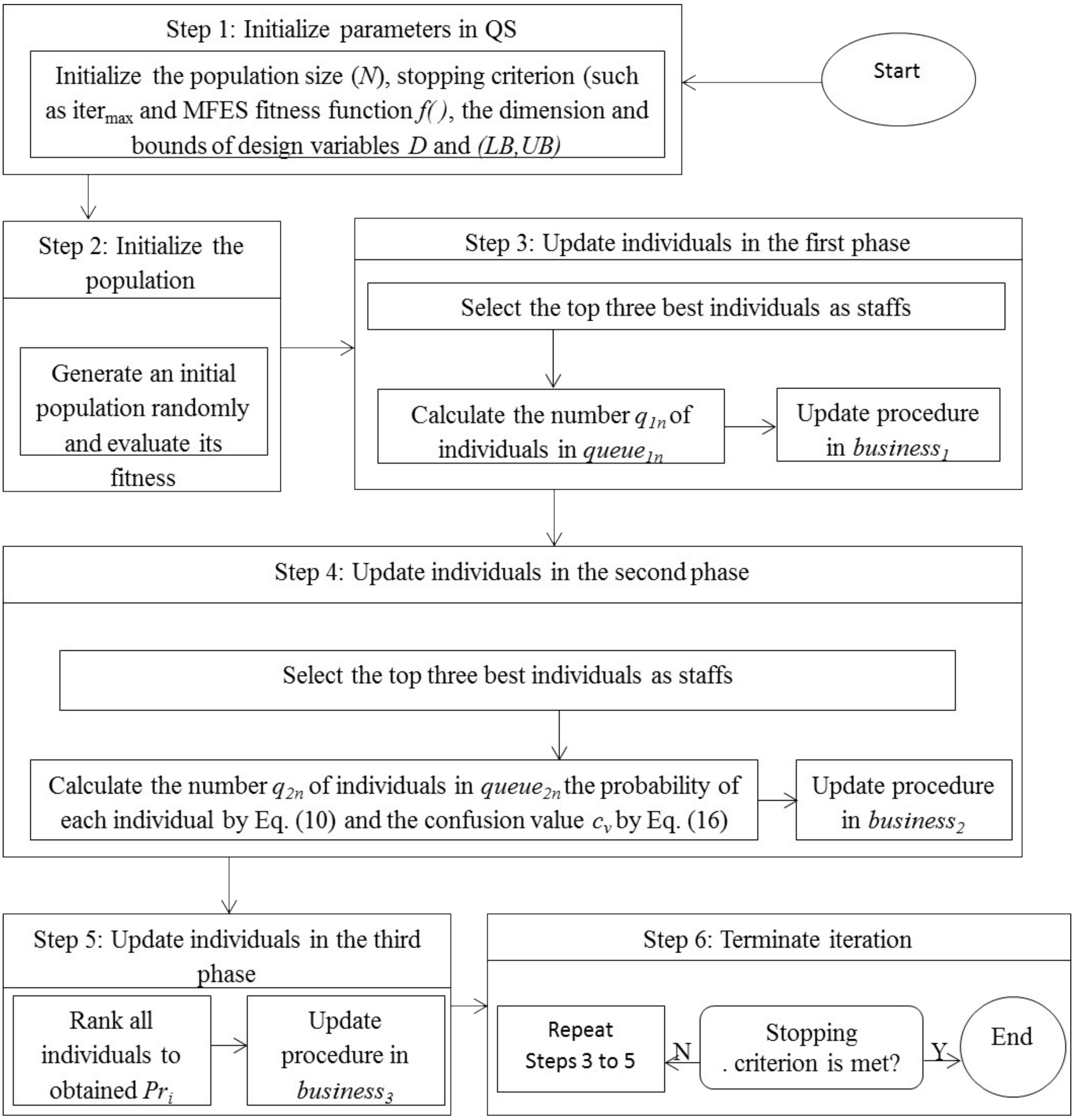

Fig S10. QSA working framework

S6 Mathematical formulation of Weights method for evaluating the relative relevance of input variables on ANN model response

$$I_J = \frac{\sum_{m=1}^{m=Nh}\left(\left(\frac{\left|w_{jm}^{ih}\right|}{\sum_{k=1}^{Ni}\left|w_{km}^{ih}\right|}\right)\times\left|w_{mn}^{ho}\right|\right)}{\sum_{k=1}^{k=Ni}\left\{\sum_{m=1}^{m=Nh}\left(\frac{\left|w_{jm}^{ij}\right|}{\sum_{k=1}^{Ni}\left|w_{km}^{ih}\right|}\right)\times\left|w_{mn}^{ho}\right|\right\}} \tag{5}$$

where I_J = relative significance of the jth input variable on the output variable,

Ni = number of input neurons

Nh = number of hidden neuron

w = connection weight;

The superscripts i, h and o = input, hidden, and output layers, respectively.

The subscripts k, m and n = number of input, hidden, and output neurons, respectively.

References

[1] W.A.H. Altowayti, H.A. Algaifi, S.A. Bakar, S. Shahir, The adsorptive removal of As (III) using biomass of arsenic resistant Bacillus thuringiensis strain WS3: characteristics and modelling studies, Ecotoxicology and Environmental Safety. 172 (2019) 176–185.

[2] M.S. Podder, C.B. Majumder, The use of artificial neural network for modelling of phycoremediation of toxic elements As (III) and As (V) from wastewater using Botryococcus braunii, Spectrochimica Acta Part A: Molecular and Biomolecular Spectroscopy. 155 (2016) 130–145.

[3] D. Ranjan, D. Mishra, S.H. Hasan, Bioadsorption of arsenic: an artificial neural networks and response surface methodological approach, Industrial & Engineering Chemistry Research. 50 (2011) 9852–9863.

[4] K.R. Raj, A. Kardam, J.K. Arora, S. Srivastava, An application of ANN modeling on the biosorption of arsenic, Waste and Biomass Valorization. 4 (2013) 401–407.

[5] B.K. Nath, C. Chaliha, E. Kalita, Iron oxide Permeated Mesoporous rice-husk nanobiochar (IPMN) mediated removal of dissolved arsenic (As): Chemometric modelling and adsorption dynamics, Journal of Environmental Management. 246 (2019) 397–409.

[6] J.A. Rodríguez-Romero, D.I. Mendoza-Castillo, H.E. Reynel-Ávila, D.A. de Haro-Del Rio, L.M. González-Rodríguez, A. Bonilla-Petriciolet, C.J. Duran-Valle, K.I. Camacho-Aguilar, Preparation of a new adsorbent for the removal of arsenic and its simulation with artificial neural network-based adsorption models, Journal of Environmental Chemical Engineering. 8 (2020) 103928.

[7] M.F. Ahmad, S. Haydar, A.A. Bhatti, A.J. Bari, Application of artificial neural network for the prediction of biosorption capacity of immobilized Bacillus subtilis for the removal of cadmium ions from aqueous solution, Biochemical Engineering Journal. 84 (2014) 83–90.

[8] G. Aditya, A. Hossain, Valorization of aquaculture waste in removal of cadmium from aqueous solution: optimization by kinetics and ANN analysis, Applied Water Science. 8 (2018) 1–14.

[9] R.S. Kiran, G.M. Madhu, S.V. Satyanarayana, P. Kalpana, G.S. Rangaiah, Applications of Box–Behnken experimental design coupled with artificial neural networks for biosorption of low concentrations of cadmium using Spirulina (Arthrospira) spp., Resource-Efficient Technologies. 3 (2017) 113–123.

[10] U. Yurtsever, M. Yurtsever, İ.A. Şengil, N. Kıratlı Yılmazçoban, Fast artificial neural network (FANN) modeling of Cd (II) ions removal by valonia resin, Desalination and Water Treatment. 56 (2015) 83–96.

[11] M. Fawzy, M. Nasr, H. Nagy, S. Helmi, Artificial intelligence and regression analysis for Cd (II) ion biosorption from aqueous solution by Gossypium barbadense waste, Environmental Science and Pollution Research. 25 (2018) 5875–5888.

[12] A. Takdastan, S. Samarbaf, Y. Tahmasebi, N. Alavi, A.A. Babaei, Alkali modified oak waste residues as a cost-effective adsorbent for enhanced removal of cadmium from water: Isotherm, kinetic, thermodynamic and artificial neural network modeling, Journal of Industrial and Engineering Chemistry. 78 (2019) 352–363.

[13] A. Kardam, K.R. Raj, J.K. Arora, M.M. Srivastava, S. Srivastava, Artificial neural network modeling for sorption of cadmium from aqueous system by shelled Moringa oleifera seed powder as an agricultural waste, Journal of Water Resource and Protection. 2 (2010) 339.

[14] M. Nasr, A.E.D. Mahmoud, M. Fawzy, A. Radwan, Artificial intelligence modeling of cadmium (II) biosorption using rice straw, Applied Water Science. 7 (2017) 823–831.

[15] S. Nag, A. Mondal, D.N. Roy, N. Bar, S.K. Das, Sustainable bioremediation of Cd (II) from aqueous solution using natural waste materials: kinetics, equilibrium, thermodynamics, toxicity studies and GA-ANN hybrid modelling, Environmental Technology & Innovation. 11 (2018) 83–104.
[16] M.R. Kowsari, H. Sepehrian, M. Mahani, J. Fasihi, Cobalt (II) adsorption from aqueous solution using alginate-SBA-15 nanocomposite: Kinetic, isotherm, thermodynamic studies and neural network modeling, Materials Focus. 5 (2016) 91–99.
[17] S. Shukla, U. Kumar, A. Prakash, V.K. Jain, An artificial neural network (ANN)-based framework for the Cr removal from the spiked water samples by chitosan oligosaccharide-coated iron oxide nanoparticles, Nanotechnology for Environmental Engineering. 2 (2017) 1–11.
[18] S. Sen, S. Nandi, S. Dutta, Application of RSM and ANN for optimization and modeling of biosorption of chromium (VI) using cyanobacterial biomass, Applied Water Science. 8 (2018) 1–12.
[19] M. Fawzy, M. Nasr, A. Abdel-Gaber, S. Fadly, Biosorption of Cr (VI) from aqueous solution using agricultural wastes, with artificial intelligence approach, Separation Science and Technology. 51 (2016) 416–426.
[20] D. Krishna, R.P. Sree, Artificial Neural Network (ANN) Approach for modeling chromium (VI) Adsorption from aqueous solution using a Borasus Flabellifer coir powder, International Journal of Applied Science and Engineering. 12 (2014) 177–192.
[21] D. Krishna, G.S. Kumar, D.R.P. Raju, Optimization of Process Parameters for the Removal of Chromium (VI) from Waste Water Using Mixed Adsorbent, International Journal of Applied Science and Engineering. 16 (2019) 187–200.
[22] K. Singh, J.K. Arora, T.J.M. Sinha, S. Srivastava, Functionalization of nanocrystalline cellulose for decontamination of Cr (III) and Cr (VI) from aqueous system: computational modeling approach, Clean Technologies and Environmental Policy. 16 (2014) 1179–1191.
[23] S. Nag, N. Bar, S.K. Das, Cr (VI) removal from aqueous solution using green adsorbents in continuous bed column–statistical and GA-ANN hybrid modelling, Chemical Engineering Science. 226 (2020) 115904.
[24] R. Beigzadeh, S.O. Rastegar, Assessment of Cr (VI) Biosorption from Aqueous Solution by Artificial Intelligence, Chemical Methodologies. 4 (2020) 181–190.
[25] V. Singh, J. Singh, V. Mishra, Development of a cost-effective, recyclable and viable metal ion doped adsorbent for simultaneous adsorption and reduction of toxic Cr (VI) ions, Journal of Environmental Chemical Engineering. 9 (2021) 105124.
[26] S. Nag, A. Mondal, N. Bar, S.K. Das, Biosorption of chromium (VI) from aqueous solutions and ANN modelling, Environmental Science and Pollution Research. 24 (2017) 18817–18835.
[27] N. Parveen, S. Zaidi, M. Danish, Development of SVR-based model and comparative analysis with MLR and ANN models for predicting the sorption capacity of Cr (VI), Process Safety and Environmental Protection. 107 (2017) 428–437.
[28] M. Shanmugaprakash, V. Sivakumar, Development of experimental design approach and ANN-based models for determination of Cr (VI) ions uptake rate from aqueous solution onto the solid biodiesel waste residue, Bioresource Technology. 148 (2013) 550–559.
[29] T. Khan, M.H. Isa, M.R.U. Mustafa, H. Yeek-Chia, L. Baloo, T.S.B. Abd Manan, M.O. Saeed, Cr (VI) adsorption from aqueous solution by an agricultural waste based carbon, RSC Advances. 6 (2016) 56365–56374.
[30] M. Solgi, T. Najib, S. Ahmadnejad, B. Nasernejad, Synthesis and characterization of novel activated carbon from Medlar seed for chromium removal: Experimental analysis

and modeling with artificial neural network and support vector regression, Resource-Efficient Technologies. 3 (2017) 236–248.
[31] V. Chakraborty, P. Das, Synthesis of nano-silica-coated biochar from thermal conversion of sawdust and its application for Cr removal: kinetic modelling using linear and nonlinear method and modelling using artificial neural network analysis, Biomass Conversion and Biorefinery. (2020) 1–11.
[32] D. Bingöl, M. Inal, S. Çetintaş, Evaluation of copper biosorption onto date palm (Phoenix dactylifera L.) seeds with MLR and ANFIS models, Industrial & Engineering Chemistry Research. 52 (2013) 4429–4435.
[33] S.G. Shandi, F.D. Ardejani, F. Sharifi, Assessment of Cu (II) removal from an aqueous solution by raw Gundelia tournefortii as a new low-cost biosorbent: Experiments and modelling, Chinese Journal of Chemical Engineering. 27 (2019) 1945–1955.
[34] H.A. Hamid, Y. Jenidi, W. Thielemans, C. Somerfield, R.L. Gomes, Predicting the capability of carboxylated cellulose nanowhiskers for the remediation of copper from water using response surface methodology (RSM) and artificial neural network (ANN) models, Industrial Crops and Products. 93 (2016) 108–120.
[35] C. Sutherland, A. Marcano, B. Chittoo, Artificial neural network-genetic algorithm prediction of heavy metal removal using a novel plant-based biosorbent banana floret: kinetic, equilibrium, thermodynamics and desorption studies, in: Desalination and Water Treatment, IntechOpen, 2018: pp. 385–411.
[36] N. Prakash, S.A. Manikandan, L. Govindarajan, V. Vijayagopal, Prediction of biosorption efficiency for the removal of copper (II) using artificial neural networks, Journal of Hazardous Materials. 152 (2008) 1268–1275.
[37] D. Podstawczyk, A. Witek-Krowiak, A. Dawiec, A. Bhatnagar, Biosorption of copper (II) ions by flax meal: empirical modeling and process optimization by response surface methodology (RSM) and artificial neural network (ANN) simulation, Ecological Engineering. 83 (2015) 364–379.
[38] N.G. Turan, B. Mesci, O. Ozgonenel, Artificial neural network (ANN) approach for modeling Zn (II) adsorption from leachate using a new biosorbent, Chemical Engineering Journal. 173 (2011) 98–105.
[39] Y.J. Wong, S.K. Arumugasamy, C.H. Chung, A. Selvarajoo, V. Sethu, Comparative study of artificial neural network (ANN), adaptive neuro-fuzzy inference system (ANFIS) and multiple linear regression (MLR) for modeling of Cu (II) adsorption from aqueous solution using biochar derived from rambutan (Nephelium lappaceum) peel, Environmental Monitoring and Assessment. 192 (2020) 1–20.
[40] K. Yadav, M. Raphi, S. Jagadevan, Adsorption of copper (II) on chemically modified biochar: A single-stage batch adsorber design and predictive modeling through artificial neural network, Biomass Conversion and Biorefinery. (2021) 1–16.
[41] P.R. Souza, G.L. Dotto, N.P.G. Salau, Artificial neural network (ANN) and adaptive neuro-fuzzy interference system (ANFIS) modelling for nickel adsorption onto agro-wastes and commercial activated carbon, Journal of Environmental Chemical Engineering. 6 (2018) 7152–7160.
[42] H. Esfandian, M. Parvini, B. Khoshandam, A. Samadi-Maybodi, Artificial neural network (ANN) technique for modeling the mercury adsorption from aqueous solution using Sargassum Bevanom algae, Desalination and Water Treatment. 57 (2016) 17206–17219.
[43] E.A. Dil, M. Ghaedi, G.R. Ghezelbash, A. Asfaram, A.M. Ghaedi, F. Mehrabi, Modeling and optimization of Hg 2+ ion biosorption by live yeast Yarrowia lipolytica 70562 from aqueous solutions under artificial neural network-genetic algorithm and

response surface methodology: kinetic and equilibrium study, RSC Advances. 6 (2016) 54149–54161.

[44] M. Pazouki, M. Zabihi, J. Shayegan, M.H. Fatehi, Mercury ion adsorption on AC@ Fe3O4-NH2-COOH from saline solutions: Experimental studies and artificial neural network modeling, Korean Journal of Chemical Engineering. 35 (2018) 671–683.

[45] S.P.G. Zaferani, M.R.S. Emami, M.K. Amiri, E. Binaeian, Optimization of the removal Pb (II) and its Gibbs free energy by thiosemicarbazide modified chitosan using RSM and ANN modeling, International Journal of Biological Macromolecules. 139 (2019) 307–319.

[46] A. Sadeghizadeh, F. Ebrahimi, M. Heydari, M. Tahmasebikohyani, F. Ebrahimi, A. Sadeghizadeh, Adsorptive removal of Pb (II) by means of hydroxyapatite/chitosan nanocomposite hybrid nanoadsorbent: ANFIS modeling and experimental study, Journal of Environmental Management. 232 (2019) 342–353.

[47] K. Yetilmezsoy, S. Demirel, Artificial neural network (ANN) approach for modeling of Pb (II) adsorption from aqueous solution by Antep pistachio (Pistacia Vera L.) shells, Journal of Hazardous Materials. 153 (2008) 1288–1300.

[48] A. Kardam, K.R. Raj, J.K. Arora, S. Srivastava, Artificial neural network modeling for biosorption of Pb (II) ions on nanocellulose fibers, Bionanoscience. 2 (2012) 153–160.

[49] A. Ronda, M.A. Martín-Lara, A.I. Almendros, A. Pérez, G. Blázquez, Comparison of two models for the biosorption of Pb (II) using untreated and chemically treated olive stone: Experimental design methodology and adaptive neural fuzzy inference system (ANFIS), Journal of the Taiwan Institute of Chemical Engineers. 54 (2015) 45–56.

[50] M. Ashrafi, H. Borzuie, G. Bagherian, M.A. Chamjangali, H. Nikoofard, Artificial neural network and multiple linear regression for modeling sorption of Pb2+ ions from aqueous solutions onto modified walnut shell, Separation Science and Technology. 55 (2020) 222–233.

[51] F. Rahimpour, T. Shojaeimehr, M. Sadeghi, Biosorption of Pb (II) using Gundelia tournefortii: Kinetics, equilibrium, and thermodynamics, Separation Science and Technology. 52 (2017) 596–607.

[52] D. Bingöl, M. Hercan, S. Elevli, E. Kılıç, Comparison of the results of response surface methodology and artificial neural network for the biosorption of lead using black cumin, Bioresource Technology. 112 (2012) 111–115.

[53] P.L. Narayana, A.K. Maurya, X.-S. Wang, M.R. Harsha, O. Srikanth, A.A. Alnuaim, W.A. Hatamleh, A.A. Hatamleh, K.K. Cho, U.M. Reddy, Artificial neural networks modeling for lead removal from aqueous solutions using iron oxide nanocomposites from bio-waste mass, Environmental Research. (2021) 111370.

[54] S. Ullah, M.A. Assiri, A.G. Al-Sehemi, M.A. Bustam, M. Sagir, F.A. Abdulkareem, M.R. Raza, M. Ayoub, A. Irfan, Characteristically insights, artificial neural network (ANN), equilibrium, and kinetic studies of Pb (II) ion adsorption on rice husks treated with nitric acid, International Journal of Environmental Research. 14 (2020) 43–60.

[55] T. Khan, M.R.U. Mustafa, M.H. Isa, T.S.B.A. Manan, Y.-C. Ho, J.-W. Lim, N.Z. Yusof, Artificial neural network (ANN) for modelling adsorption of lead (Pb (II)) from aqueous solution, Water, Air, & Soil Pollution. 228 (2017) 1–15.

[56] A.A. Oladipo, M. Gazi, Nickel removal from aqueous solutions by alginate-based composite beads: Central composite design and artificial neural network modeling, Journal of Water Process Engineering. 8 (2015) e81–e91.

[57] M. Fawzy, M. Nasr, S. Adel, S. Helmi, Regression model, artificial neural network, and cost estimation for biosorption of Ni (II)-ions from aqueous solutions by Potamogeton pectinatus, International Journal of Phytoremediation. 20 (2018) 321–329.

[58] B.R. Broujeni, A. Nilchi, F. Azadi, Adsorption modeling and optimization of thorium (IV) ion from aqueous solution using chitosan/TiO2 nanocomposite: Application of artificial neural network and genetic algorithm, Environmental Nanotechnology, Monitoring & Management. 15 (2021) 100400.
[59] H. Heshmati, M. Torab-Mostaedi, H. Ghanadzadeh Gilani, A. Heydari, Kinetic, isotherm, and thermodynamic investigations of uranium (VI) adsorption on synthesized ion-exchange chelating resin and prediction with an artificial neural network, Desalination and Water Treatment. 55 (2015) 1076–1087.
[60] M. Zhu, F. Li, W. Chen, X. Yin, Z. Yi, S. Zhang, Adsorption of U (VI) from aqueous solution by using KMnO4-modified hazelnut shell activated carbon: characterisation and artificial neural network modelling, Environmental Science and Pollution Research. 28 (2021) 47354–47366.
[61] S. Yildiz, Artificial neural network (ANN) approach for modeling Zn (II) adsorption in batch process, Korean Journal of Chemical Engineering. 34 (2017) 2423–2434.
[62] M. Shanmugaprakash, S. Venkatachalam, K. Rajendran, A. Pugazhendhi, Biosorptive removal of Zn (II) ions by Pongamia oil cake (Pongamia pinnata) in batch and fixed-bed column studies using response surface methodology and artificial neural network, Journal of Environmental Management. 227 (2018) 216–228.
[63] S. Ullah, M.A. Assiri, M.A. Bustam, A.G. Al-Sehemi, F.A. Abdul Kareem, A. Irfan, Equilibrium, kinetics and artificial intelligence characteristic analysis for Zn (II) ion adsorption on rice husks digested with nitric acid, Paddy and Water Environment. 18 (2020) 455–468.
[64] A. Esmaeili, A.A. Beni, Novel membrane reactor design for heavy-metal removal by alginate nanoparticles, Journal of Industrial and Engineering Chemistry. 26 (2015) 122–128.
[65] E. Allahkarami, A. Igder, A. Fazlavi, B. Rezai, Prediction of Co (II) and Ni (II) ions removal from wastewater using artificial neural network and multiple regression models, Physicochemical Problems of Mineral Processing. 53 (2017).
[66] R. Khandanlou, H.R.F. Masoumi, M.B. Ahmad, K. Shameli, M. Basri, K. Kalantari, Enhancement of heavy metals sorption via nanocomposites of rice straw and Fe3O4 nanoparticles using artificial neural network (ANN), Ecological Engineering. 91 (2016) 249–256.
[67] M. Fawzy, M. Nasr, S. Adel, H. Nagy, S. Helmi, Environmental approach and artificial intelligence for Ni (II) and Cd (II) biosorption from aqueous solution using Typha domingensis biomass, Ecological Engineering. 95 (2016) 743–752.
[68] M.R. Fagundes-Klen, P. Ferri, T.D. Martins, C.R.G. Tavares, E.A. Silva, Equilibrium study of the binary mixture of cadmium–zinc ions biosorption by the Sargassum filipendula species using adsorption isotherms models and neural network, Biochemical Engineering Journal. 34 (2007) 136–146.
[69] S. Rebouh, M. Bouhedda, S. Hanini, Neuro-fuzzy modeling of Cu (II) and Cr (VI) adsorption from aqueous solution by wheat straw, Desalination and Water Treatment. 57 (2016) 6515–6530.
[70] S. Varshney, P. Jain, J.K. Arora, S. Srivastava, Process development for the removal of toxic metals by functionalized wood pulp: kinetic, thermodynamic, and computational modeling approach, Clean Technologies and Environmental Policy. 18 (2016) 2613–2623.
[71] D.I. Mendoza-Castillo, H.E. Reynel-Ávila, F.J. Sánchez-Ruiz, R. Trejo-Valencia, J.E. Jaime-Leal, A. Bonilla-Petriciolet, Insights and pitfalls of artificial neural network modeling of competitive multi-metallic adsorption data, Journal of Molecular Liquids. 251 (2018) 15–27.

[72] H.E. Reynel-Avila, A. Bonilla-Petriciolet, G. de la Rosa, Analysis and modeling of multicomponent sorption of heavy metals on chicken feathers using Taguchi's experimental designs and artificial neural networks, Desalination and Water Treatment. 55 (2015) 1885–1899.
[73] A.H. Hamidian, S. Esfandeh, Y. Zhang, M. Yang, Simulation and optimization of nanomaterials application for heavy metal removal from aqueous solutions, Inorganic and Nano-Metal Chemistry. 49 (2019) 217–230.
[74] A.A. Prabhu, S. Chityala, D. Jayachandran, N.N. Deshavath, V.D. Veeranki, A two step optimization approach for maximizing biosorption of hexavalent chromium ions (Cr (VI)) using alginate immobilized Sargassum sp in a packed bed column, Separation Science and Technology. 56 (2021) 90–106.
[75] M. Banerjee, N. Bar, R.K. Basu, S.K. Das, Comparative study of adsorptive removal of Cr (VI) ion from aqueous solution in fixed bed column by peanut shell and almond shell using empirical models and ANN, Environmental Science and Pollution Research. 24 (2017) 10604–10620.
[76] E. Oguz, M. Ersoy, Biosorption of cobalt (II) with sunflower biomass from aqueous solutions in a fixed bed column and neural networks modelling, Ecotoxicology and Environmental Safety. 99 (2014) 54–60.
[77] M. Banerjee, N. Bar, S.K. Das, Cu (II) removal from aqueous solution using the walnut shell: adsorption study, regeneration study, plant scale-up design, economic feasibility, statistical, and GA-ANN modeling, International Journal of Environmental Research. 15 (2021) 875–891.
[78] M. Khajeh, E. Jahanbin, Application of cuckoo optimization algorithm–artificial neural network method of zinc oxide nanoparticles–chitosan for extraction of uranium from water samples, Chemometrics and Intelligent Laboratory Systems. 135 (2014) 70–75.
[79] E. Tomczak, Application of ANN and EA for description of metal ions sorption on chitosan foamed structure—Equilibrium and dynamics of packed column, Computers & Chemical Engineering. 35 (2011) 226–235.
[80] L.T. Popoola, Nano-magnetic walnut shell-rice husk for Cd (II) sorption: design and optimization using artificial intelligence and design expert, Heliyon. 5 (2019) e02381.
[81] P.J. Braspenning, F. Thuijsman, A.J.M.M. Weijters, Artificial neural networks: an introduction to ANN theory and practice, Springer Science & Business Media, 1995.
[82] E. Oguz, M. Ersoy, Removal of Cu2+ from aqueous solution by adsorption in a fixed bed column and Neural Network Modelling, Chemical Engineering Journal. 164 (2010) 56–62.
[83] M. Banerjee, N. Bar, S.K. Das, Cu (II) removal from aqueous solution using the walnut shell: adsorption study, regeneration study, plant scale-up design, economic feasibility, statistical, and GA-ANN modeling, International Journal of Environmental Research. 15 (2021) 875–891.
[84] S. Ullah, M.A. Assiri, A.G. Al-Sehemi, M.A. Bustam, M. Sagir, F.A. Abdulkareem, M.R. Raza, M. Ayoub, A. Irfan, Characteristically insights, artificial neural network (ANN), equilibrium, and kinetic studies of Pb (II) ion adsorption on rice husks treated with nitric acid, International Journal of Environmental Research. 14 (2020) 43–60.
[85] P. Moradi, S. Hayati, T. Ghahrizadeh, Modeling and optimization of lead and cobalt biosorption from water with Rafsanjan pistachio shell, using experiment based models of ANN and GP, and the grey wolf optimizer, Chemometrics and Intelligent Laboratory Systems. 202 (2020) 104041.
[86] D.I. Mendoza-Castillo, N. Villalobos-Ortega, A. Bonilla-Petriciolet, J.C. Tapia-Picazo, Neural network modeling of heavy metal sorption on lignocellulosic biomasses: effect

of metallic ion properties and sorbent characteristics, Industrial & Engineering Chemistry Research. 54 (2015) 443–453.
[87] M. Dolatabadi, M. Mehrabpour, M. Esfandyari, H. Alidadi, M. Davoudi, Modeling of simultaneous adsorption of dye and metal ion by sawdust from aqueous solution using of ANN and ANFIS, Chemometrics and Intelligent Laboratory Systems. 181 (2018) 72–78. https://doi.org/10.1016/j.chemolab.2018.07.012.
[88] A. Ghosh, K. Sinha, P.D. Saha, Central composite design optimization and artificial neural network modeling of copper removal by chemically modified orange peel, Desalination and Water Treatment. 51 (2013) 7791–7799.
[89] B. Singha, N. Bar, S.K. Das, The use of artificial neural networks (ANN) for modeling of adsorption of Cr (VI) ions, Desalination and Water Treatment. 52 (2014) 415–425.